Bachelor thesis

# Optimization of sample preparation and first measurements in a study on the dynamics of G-quadruplex DNA

Utrecht University

July 6, 2013

*Author:*
Rosalinde Pots
3471586

*Supervisor:*
Dr. Gerhard Blab

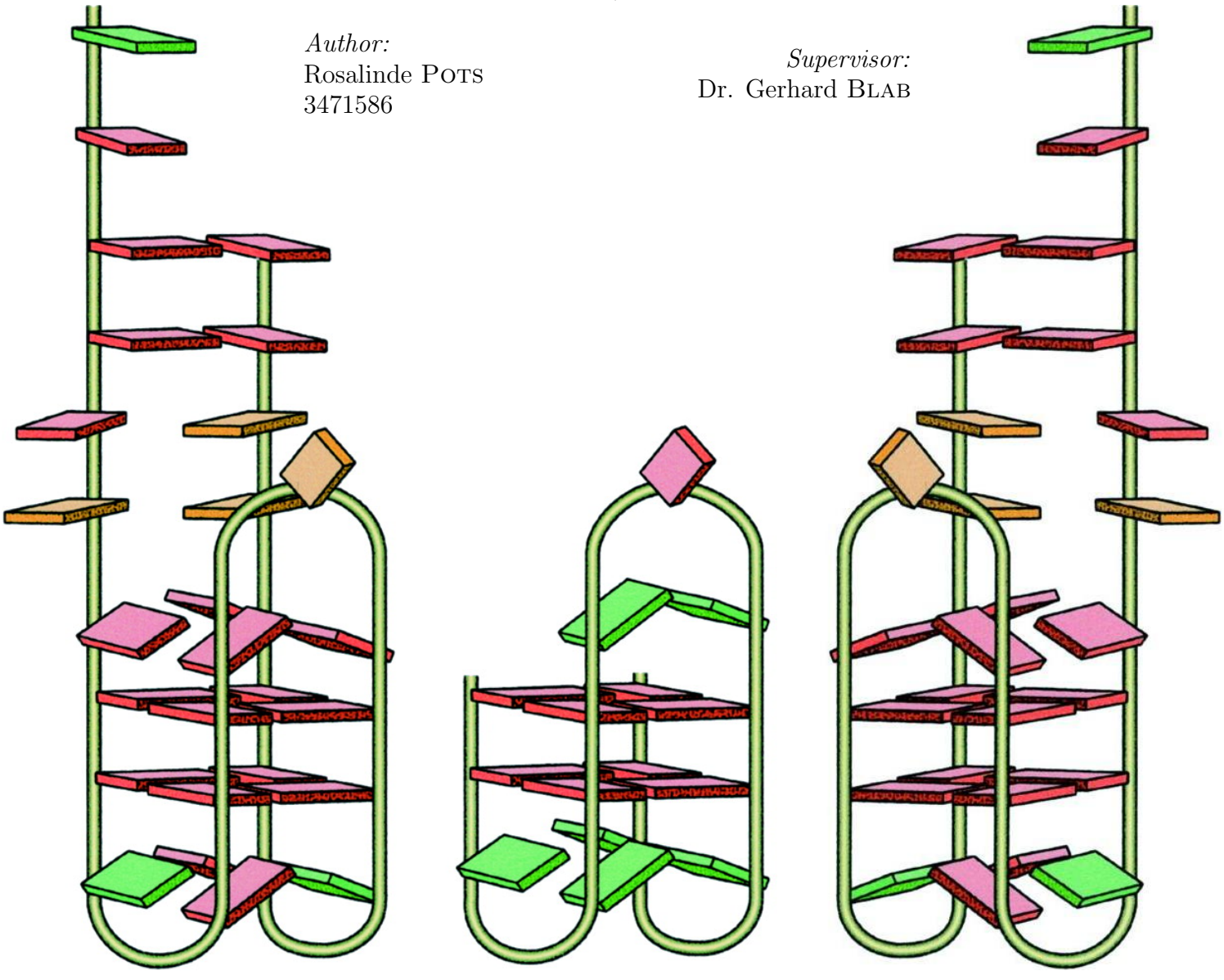

Siddiqui-Jain et al., *PNAS*, 2002

# Contents

# Chapter 1

# Introduction

The G-quadruplex structure is, in contrast to the double helix structure, a four-stranded structure and is formed out of single-stranded DNA that is rich in the nucleobase guanine. The first clues for the possible different structure of guanine rich DNA was given by Ivar Bang in 1910. He observed a strange gel formation by guanylic acid (after first neutralizing it with KOH and then re-acidifying with acetic acid)[1]. Unfortunately he did not draw the right conclusions and thought this gel formation was evidence for some kind of new nucleic acid.

It took scientists over half a century to discover the true reason for the gel-formation. In 1962 Martin Gellert and colleagues published a paper in which they stated that the gel-formation of guanylic acid was due to the formation of a structure different from the double helix structure discovered 9 years before[2]. They used the fibre x-ray diffraction patterns to analyze the new structure. The structure is called G-quadruplex, which is a four-stranded structure consisting of stacked planes, each formed by 4 guanines.

This structure, long time thought of as an in vitro phenomenon, can form in several parts of the DNA. Important are the various DNA sequences in the telomeres and in promoters for which G-quadruplex forming is possible, because of their possible involvement with a variety of diseases like diabetes type 1 and several types of cancer[3][4]. This could have huge potentials for the understanding of the expression of certain genes and also for the development of anti-cancer drugs, which is the reason why there is so much research on the properties of G-quadruplex DNA. The suppressing influence of G-Quadruplexes on the activity of the enzyme telomerase has been confirmed. Recent studies even have shown G-quadruplex forming in human cells, in telomeres as well as in other parts of the DNA[5].

In this study we will focus on the dynamical behavior of G-quadruplexes and the influence of the exertion of forces from the small force regime on that behavior. We will use a centrifugal force microscope for the DNA manipulation, which can measure a big amount of molecules at the same time. We will optimize the sample preparation for the setup and we will analyze telomere DNA and ILPR (insulin linked polymorphic region), which is a regulatory sequence of the insulin gene.

# Chapter 2

# Theoretical Background

## 2.1 G-Quadruplex

The best known and most occurring structure of DNA is the double-helix structure. This structure has two anti-parallel DNA-strands twisted around each other. It has a backbone consisting of a sugar group and a phosphate group for each nucleobase to which it is attached. The nucleobases adenine and thymine and the bases cytosine and guanine will form hydrogen bonds with each other, through which the two strands of DNA are connected (figure 2.1A). But apart from this structure, there are several other conformations of DNA. One of the most important alternate DNA structures is G-quadruplex DNA.

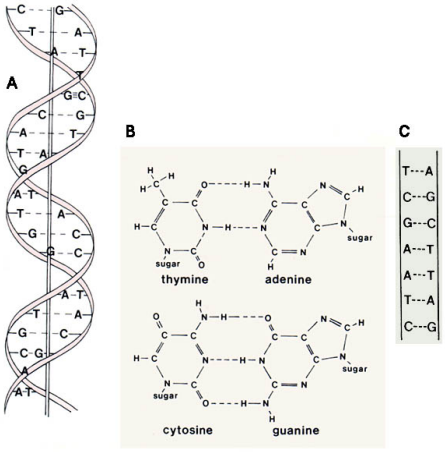


Figure 2.1: *A: DNA in double-stranded helix structure. B and C: the bonds between the four different base pairs. (picture from [6])*

### 2.1.1 Structure

G-quadruplexes occur in DNA rich in guanine. This is because the structures stability is based on the unique property of guanine to form four hydrogen bounds. The G-quadruplexes consist of stacked planes. Each plane, called G-quartet, consists of four guanines arranged as in figure 2.2 *A*. The planes are stable only if there is a monovalent cation, which is most of the time a $K^+$, but can also be $Na^+$, $Rb^+$ and many more. This cation is necessary to neutralize the negative charge caused by the inwards positioned oxygen.

Every guanine in the G-quartet is connected to the guanine situated above and/or below it by a backbone, as shown in figure 2.2 *B*. There are several confirmations of G-quadruplexes, of which some examples are shown in figure 2.2 *B*.

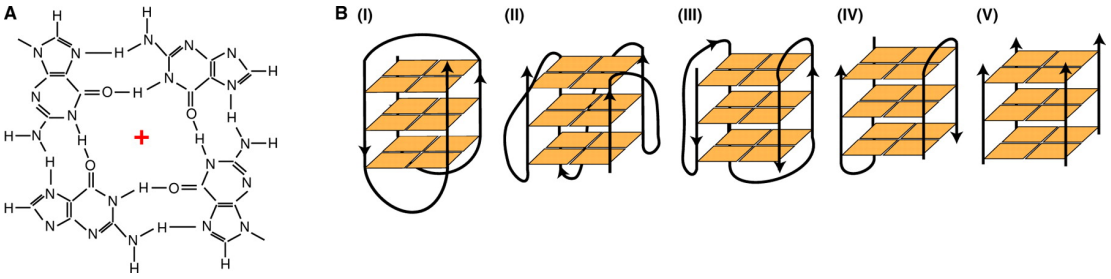


Figure 2.2: *A: a G-quartet with a monovalent cation in the middle. (picture from [7]) B:Different G-quadruplex conformations. (I) monomolecular antiparallel G-quadruplex, (II) monomolecular parallel G-quadruplex, (III) hybrid monomolecular G-quadruplex, (IV) bimolecular anti-parallel G-quadruplex, (V) intramolecular parallel G-quadruplex. (picture from [7])*

The different quadruplexes can be classified by the number of DNA strands participating in de structure. For instance the quadruplex in figure 2.2 *B(V)* is an example of an intermolecular quadruplex consisting of four DNA strands. Figure 2.2 *B(IV)* is an intermolecular quadruplex consisting of two DNA strands and figure 2.2 *B(I), B(II) and B(III)* are all examples of intramolecular quadruplexes (consisting of only one DNA strand). Also the four different strands, whether they consist of one DNA strand or more, can be parallel or anti-parallel or a hybrid form. So for the parallel variant the four strands go in the same direction (figure 2.2 *B(I) and B(IV)*). In the anti-parallel form, two strands will be in one direction and two in the other direction. Here the strands going in the same direction can be adjacent as in figure 2.2 *B(I)* or they can be opposite like in figure 2.2 *B(IV)*. In a hybrid form three of the strands will be in the same direction and one will be in the other direction, like in figure 2.2 *B(III)*.

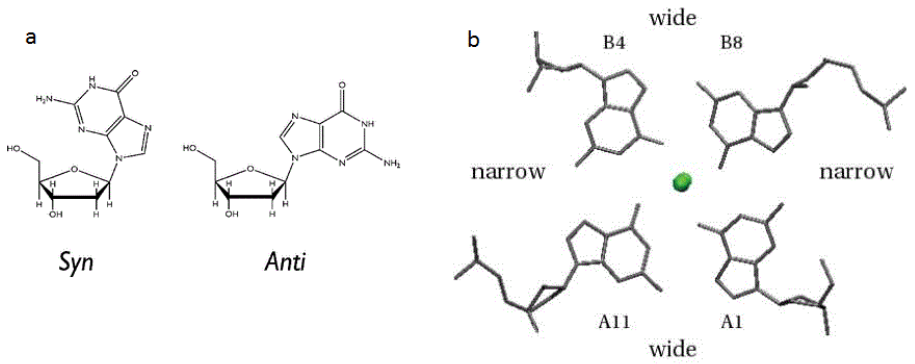


Figure 2.3: *a: syn- and anti-conformation of the bond between the guanine and the sugar.(picture from [3]) b: the arrangement of the guanines in a G-quartet, also showing the conformation of the guanine with respect to the sugar and the effect of that conformation on the width of the grooves. (picture from [8])*

Whether the strands are parallel, anti-parallel or hybrid determines the conformation of the guanine base with respect to the sugar. This could be either *syn* or *anti*, ensuring the hydrogen bonds can be formed correctly (figure 2.3 *a*). If all strands have the same direction, then the molecules will have the same conformation. But if this is not the case, there will be different conformations, resulting in difference in the size of the grooves between the backbones (figure 2.3 *b*).

Which structure de G-quadruplex will adopt is influenced by for instance the DNA sequence and the cation, for example potassium favors parallel conformations, but these are only influences which makes it difficult to predict what form a quadruplex will take.

It is important to realize while viewing images of G-quadruplexes that most of the time the backbones are depicted as going straight up or down, but this is only for convenience. The G-quadruplex structure is in fact a helical structure, just like the double-stranded helix structure. Figure 2.4 shows a picture of the helical structure of a quadruplex which has the same conformation as the one in figure 2.2 *B(IV)*. [3][4][8]

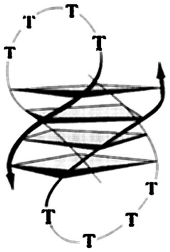

Figure 2.4: *The helical structure of a G-quadruplex. (picture from [9])*

### 2.1.2 Functions

The most basic condition for a G-quadruplex to form is of course the DNA sequence of a couple of guanines in a row repeated four times and with not to many nucleobases in between. Through this criterion there are identified 376.000 possible candidates for intramolecular G-quadruplexes in the human genome[3], although this doesn't necessarily mean that all these sites actually form quadruplexes. Still this number of potential quadruplexes is less then would be expected by chance. Also remarkable is the length and sequence of the parts in between the repeating guanines, that are the loop regions of the quadruplex[4].

Quite interesting is the distribution of the quadruplexes through the genome. For instance 43% of the genes have putative G-quadruplexes in their promoter region, which is more then expected based on the rest of the genome. This suggests that the quadruplexes have some sort of regulatory function in the transcription of the genes (figure 2.5). The fact that 67% of the genes involved with cancer have possible G-quadruplexes in their promoters, affirms this thought. Also quadruplexes are significantly under-represented in tumor suppressor genes and genes involved with protein biosynthesis and immune response. Over-expression of the oncogene c-MYC, which is involved in the transcription of about 15% of the human genes, is associated with a wide range of cancers. Because of that it has been examined thoroughly. It turned out that by destabilizing the G-quadruplex in the promoter of c-MYC, the transcription

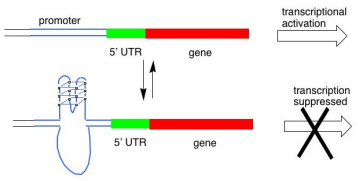


Figure 2.5: *A promotor without and with a G-quadruplex in the coding DNA strand. (picture from [10])*

of the gene tripled. It is suggested that the regulating role of this quadruplex is mediated by the protein nucleolin, which binds to this particular quadruplex. And c-MYC is only one example.

Telomeres are long non-coding parts at the endings of chromosomes, consisting of a repeated sequence, which is $GGGTTA$ for all vertebrates. During replication it is not possible to duplicate the ends, resulting in shortening of the chromosome every time it is replicated i.e. during cell division. Telomeres protect the coding parts of the DNA against this phenomenon, but this also means that every cell can only divide a certain amount of times. Even though this may sound like a mechanism which lowers the life expectancy of an organism, it actually functions as a defense mechanism against cancer. After a while the unconstrained division of cancer cells will lead to so much damage to the chromosomes that they will simply not be able to function properly anymore. However there is a enzyme called telomerase, which adds repeats to the existing telomeres (figure 2.6). Hereby it protects the chromosomes, but also gives possibilities for cancer cells to develop. And indeed in around 85% of the cancers, the cancerous cells have surpassed the normal limit on cell division by expression of telomerase. Nonetheless because of the repeating sequence containing three guanines in a row, the telomeres can spontaneously fold into quadruplexes. It is shown that when the telomere is folded into a quadruplex structure, the telomerase will not be able to elongate it.

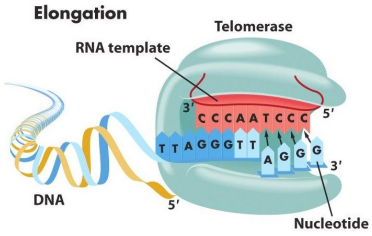


Figure 2.6: *Elongation of the telomere by telomerase. (picture from [11])*

The above described functions of the G-quadruplexes have made them an excellent subject for study in order to learn more about gene expression and also for research on anti-cancer drugs. Still it is proven to be quite difficult to develop proteins or other drugs that only target specific quadruplexes.

A recent study has prevailed that a huge amount of G-quadruplexes are actually formed in human, or more general in mammalian, cells. This study also shows that most of the quadruplexes (82.4%) are situated outside the telomeres, as is shown in figure 2.7[5]. To actually show G-quadruplexes in human cells, which they did with fluorescent structural specific antibodies, is a huge step forward. Now we know that at least a part of the sequences suitable for G-quadruplexes actually fold into G-quadruplexes.

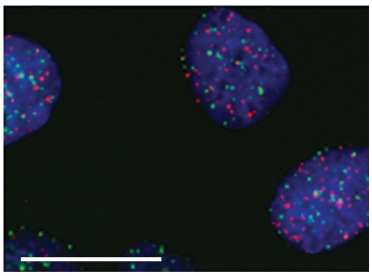

Figure 2.7: *Human cells with G-quadruplexes labeled red and telomeres labeled green, showing that the G-quadruplexes exist largely outside the telomeres. (picture from [5])*

Another part where G-quadruplexes could be of great influence, is in RNA. G-quadruplexes in RNA are more stable then in DNA, also because the RNA can not adopt the double-helix structure due to consisting of only one strand. Here the quadruplexes could play a regulatory role in the translation of the mRNA. It is even shown that

if the forming of G-quadruplexes in the mRNA of the signal transduction gene NRAS is suppressed, the translation efficiency will be four times higher.

One of the many other suggestions on the function of G-quadruplexes is that it would play a role in aligning the sister chromatids during the process of meiosis[3][4].

### 2.1.3 Methods and Instruments used in Studies

Two very important methods to study G-quadruplexes are NMR and X-ray crystallography, both have its advantages and disadvantages. However both techniques will merely say something about the structure of the quadruplex. To really observe the folding and unfolding of a G-quadruplex, other techniques are necessary. One possible technique is fluorescence resonance energy transfer or FRET. This method uses a pair of dyes. The first dye will be excited and can emit the energy through fluorescent emission. However when the second dye is in the proximity of the first, the first dye could also transfer its energy in a non-radiative fashion to the second dye. This second dye will then emit its energy through fluorescent emission at a higher wavelength then the first would. The efficiency of the energy transfer depends on the distance between the two dyes. Attaching the two distinct dyes each at another end of the quadruplex, will show you dynamics of the structure. Another way is to attach a bead to one end of the quadruplex and the other end to a piece of glass or to another bead. Now one could try to make the beads observable.[3][4][8]

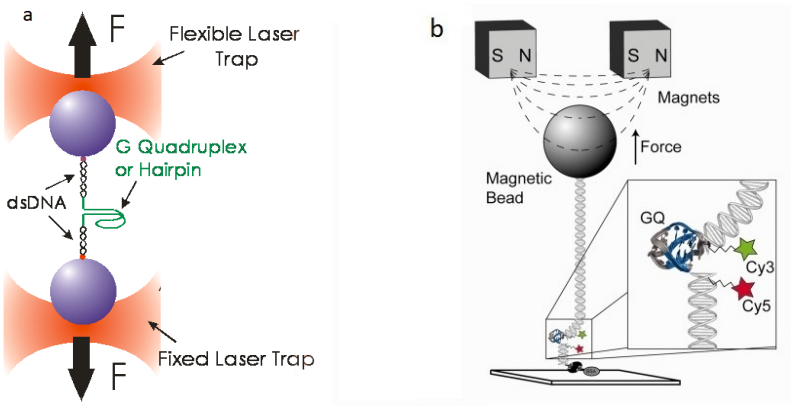


Figure 2.8: *a: optical tweezers exerting a force on two beads with a hairpin DNA structure in between. (picture from [12]) b: magnetic tweezers exerting a force on a tethered bead, using FRET to observe the dynamical behavior of the G-quadruplex. (picture from [13])*

When examining dynamics of the G-quadruplex, which is what we will be doing in this experiment, it is interesting to exert a force on the quadruplex. It is possible to use optical tweezers, which will trap the beads (or one bead if the other side is attached to for instance a coverslip)in a light beam. When moving the two light beams away from each other (or the one beam away from the coverslip), a force is exerted on the quadruplex, see figure 2.8*a*. A somewhat

similar way but using another physical principle, is using magnetic tweezers, see figure 2.8*b*. For this method obviously magnetic beads are needed and using magnetic attraction the G-quadruplex will experience a force.

A somewhat different approach is the use of a centrifugal force microscope or CFM. As the name indicates, this microscope uses the centrifugal force to exert a force on the G-quadruplex.

## 2.2 Centrifugal Force Microscopy

### 2.2.1 CFM

As indicated above the CFM uses the centrifugal force to exert a force on the G-quadruplex. Therefore the sample will be placed on an arm that can rotate. On that same arm is also the microscope attached, hence it is possible to look at the sample while rotating. The arm of the CFM consists of, going outward, a camera, an objective, a movable sample holder, an LED and a piezo (see figure 2.9a). Samples for this setup will consist of a coverslip with one end of the molecule to be examined attached to it, the other end of the molecule should be attached to a bead. Most of the time there is some coverage, for instance a microscope slide, so the molecules can be observed in a solution. If the sample is place perpendicular to the arm of the CFM, the bead will experience a centrifugal force and thus exert an equal force on the molecule. When the molecule stretches or folds, the bead will change in position. This change in position will result in a change of focus on the bead made (see figure 2.9b). When the bead will go out of focus, the size of the bead will change, as will the distribution of the light coming of the bead.

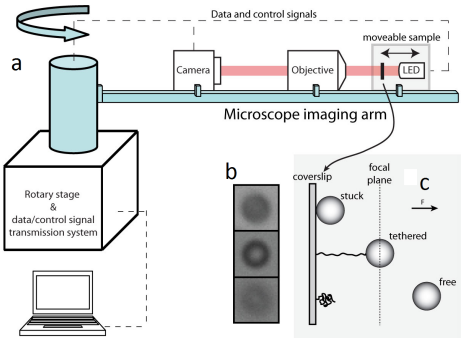


Figure 2.9: *a: experimental setup of a CFM. (picture from [14]) b: pictures of (from above) a stuck bead, a tethered bead and a free bead. (picture from [14]) c: representation of (from above) a stuck bead, a tethered bead and a free bead. (picture from [14])*

The amount of force exerted on the bead, which is equal to the force exerted on the DNA is:

$$F_c = \Delta m \omega^2 R = (\rho_{bead} - \rho_{medium}) \frac{\pi}{6} d^3 R \omega^2 \tag{2.1}$$

In this equation $\Delta m$ stands for the buoyant mass, $R$ stands for the length of the rotating arm, $\omega$ stands for the angular velocity, $\rho$ stands for the density and $d$ stands for the diameter of the used bead. In experiments on the behavior of DNA forces are used ranging from femtonewtons to piconewtons, although one would need heavy beads to exert a force in the last range.

In our setup the camera is connected to the computer via a Gigabyte Ethernet connection. The camera produces an image of $2448 \times 2050$ pixels, each pixel of the produced image $172 \times 172$nm[15]. The motor of the setup can reach

an speed of 600 rpm, but is currently limited to 200 rpm because of possible vibrations in the arm or setup. Though the intention is to raise the limit after fine-tuning.

### 2.2.2 Advantages of CFM

The CFM has several advantages over techniques like optical tweezers and magnetic tweezers.

First of all the CFM can measure in a very wide force range. Not only is it possible to vary the speed of the rotation, also it is possible to use beads of a different size or density (see equation 2.1). This way it is very easy to exert a wide range of forces with the same setup.

Another important aspect is that the force field is constant through the entire sample and will not change under folding/unfolding of the tether. This is due to the fact that the length of the tether is very small compared to the distance between the sample and the middle point of the setup. As long as the same beads are used, the force only depends on the rotation speed.

Also an important aspect is that the CFM is a relatively cheap setup, while tweezers are quite expensive.

The most important advantage of the CFM is that, unlike tweezers, it can measure several molecules at the same time. Since theoretically it is possible to measure every isolated bead in a sample, with a good sample one could be able to measure thousands of molecules at the same time.[14]

A disadvantage of the CFM is that one is limited by the high-speed rotation of the arm. Because of that one is limited to small equipment that is small and light, which also applies for the camera, and everything should be completely stable and non-moving in order to prevent unwanted vibrations in the arm.

### 2.2.3 Tethers in CFM

For measurements with the CFM on a molecule, a sample with tethers containing this molecule is needed. This means that the molecule should be attached to a coverslip with one end and to a bead with the other end, as in figure 2.10. When using DNA most of the time "handles" made from another kind of DNA are used. Usually one of the ends is attached using a biotin-streptavidin bond, which is a ligand bond, and the other end using a digoxigenin-antidigoxigenin bond, which is a antigen-antibody bond. Which of these two is used for the attachment to the bead or to the coverslip mostly depends on what kind of coating for the beads is available. These bonds both have a very high affinity, the digoxigenin-antidigoxigenin bond has an dissociation constant of about $10^{-9}$ mol/L and the biotin-streptavidin of about $10^{-14}$ mol/L, where the dissociation constant gives the propensity of a molecule or complex to separate reversibly into smaller components. These bonds are really strong and are also

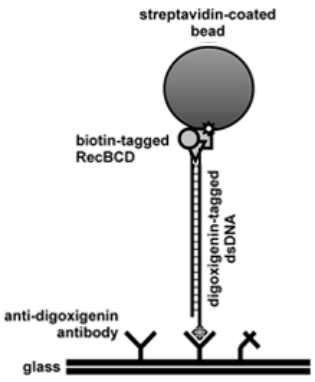


Figure 2.10: *Schematic representation of a tethered bead. (picture from [16])*

used in force measurements with double helix structure DNA, where they withstand forces of around 60 pN. The biotin-streptavidin bond can even stand more then 80 pN, also dependant of the time in which the force is exerted.[17]

When the bead really is tethered, it is possible to see the Brownian motion of the bead. How much movement this is, depends on the length of the tether. When the bead does not move, it is probably stuck to the surface. Therefore this is called a stuck bead.

When a bead is stuck instead of tethered, this is due to non-specific bounds with the coverslip. These non-specific bonds have a low affinity with a typical dissociation constant of about $10^{-6}$ mol/L. This means these kind of bonds are relatively weak compared to the bonds mentioned above. Still when there are a lot of non-specific bonds between the surface of the bead and the coverslip, the total dissociation constant will be less making the total bond stronger.

# Chapter 3

# Methods

## 3.1 DNA and Tether used in this Experiment

The two types of DNA used in this study are telomere DNA and ILPR. ILPR, standing for Insulin Linked Polymorphic Region, is a regulatory sequence for the gene coding for insulin, starting 363 base-pairs upstream the insulin gene. A locus for insulin-dependent diabetes mellitus, or better known as diabetes type 1, has been mapped to this part of the DNA, which makes it very interesting to analyze this putative G-quadruplex.[17][18] Telomeres are already discussed in subsection 2.1.2. The sequences of these two are presented in the table below, but note that these DNA strands are single-stranded.

| | |
|---|---|
| Telomere | AGCTCTCTAGA$(TTAGGG)_{12}$AGATCTCAGCT |
| ILPR | AGCTCTCTAGA$(ACAGGGGTGTGGGG)_2$AGATCTCAGCT |

From this table it is clear that the telomere has a repeat of 3 guanines in a row, which means the G-quadruplexes formed will consist of 3 planes. Because the sequence is repeated 12 times and every quadruplex uses 4 repeats (it is a four-stranded structure), the telomere can form 3 quadruplexes in a row. The ILPR will form only 1 quadruplex, but consisting of 4 planes.

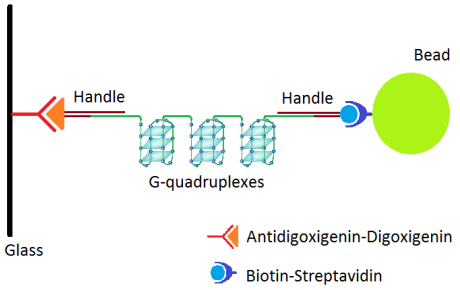


Figure 3.1: *Schematic representation of the tethered bead complex used in this study.*

To be able to make a tether out of the DNA strands, the ends of the DNA strands, or to be more specific the sequence $AGCT$, are connected to a "handle" made out of DNA. In order to make that handle, a double-stranded DNA strand from a plasmid (a $pUC18$ plasmid) is used. With the right primers, the biotin is attached to one side and digoxigenin to the other side. In order to place the quadruplex, the middle part of the DNA strand obtained from the plasmid is cut in such a way that two single-stranded parts of the DNA still stick out. These single-stranded

parts of the DNA of the plasmid have the sequence $TCGA$, which binds to the endings of the G-quadruplex DNA strand, which has the sequence $AGCT$. Then the handle with the biotin attached can bind to the streptavidin coated beads used in this experiment and the handle with digoxigenin can bind to a surface if it is incubated with antidigoxigenin. This completes the tethers that are made during this experiment, as illustrated in figure 3.1.

The DNA used in the sample preparation already contains the DNA with the handles and the biotin and digoxigenin attached. The handles consist of about 210 base pairs each, which gives them a length of about 70 nm. The length of the telomere (including handles) is about 159 nm when folded and about 225 nm when unfolded, ILPR (including handles) is about 155 nm when folded and about 181 nm when unfolded. This means that the elongation by unfolding of the telomere is about 66 nm, which is relatively large compared to the 26 nm elongation by the unfolding of ILPR. This is due to the fact that the telomere contains three quadruplexes and ILPR contains only one. As a consequence it should be easier to observe the unfolding of the telomere. This is why in this experiment the telomere will be used to optimize the sample, the setup and the analyzing programmes and ILPR will be used when it is possible to observe the unfolding of the telomere.

## 3.2 Sample Preparation: Existing Protocol

Prior to this bachelor study, a protocol for the sample was already developed although it was not perfect yet. The protocol states:

First an empty sample is made. For this a coverslip and a microscope slide are cleaned with ethanol afterwards with demineralized water and then it is blown dry with nitrogen. Next a piece of parafilm is cut with the dimensions 26 mm x 34 mm with in the middle a channel with the dimension 5 mm x 25 mm. This piece of parafilm is put on the microscope slide with the coverslip centred on top of the parafilm, as shown in figure 3.2. Then the sample is heated until the parafilm is melted. During the heating the coverslip is pressed to the surface of the microscope slide to insure it is completely attached with parafilm.

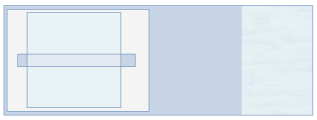

Figure 3.2: *Schematic representation of an empty sample.*

When the empty sample has cooled down again, it is filled with PTC, which is a buffer containing 20 mM Tris, 130 mM KCl, 4 mM $MgCl_2$, 0.1 mM EDTA, 20 $\mu$g/ml BSA and 80 $\mu$g/ml Heparin at pH 8. Then the sample is filled with an antidigoxigenin solution made of 15 $\mu$l PTC and 5 $\mu$l antidigoxigenin stock solution, which is 100 $\mu$g antidigoxigenin per ml PBS (phosphate buffer at pH 8). Solution is added to the sample by pipetting the solution, bit by bit, on one side of the channel and absorbing it with a tissue on the other side of the channel. It is important that no air gets in the channel, because of the risk of the formation of bubbles. After adding the antidigoxigenin solution, the sample is put upside down and left to incubate for 20 minutes. This antibody coating on the coverslip will make sure that the digoxigenin ending of the DNA strand will be able to bind to the coverslip. After incubation the channel is washed

with 2 times 75 $\mu$l PTC.

While incubating, a bead solution is made. In the case of a sample with DNA this bead solution contains 24 $\mu$l PTC and 5 $\mu$l beads, in the case of a sample without DNA this bead solution contains 25 $\mu$l PTC and 5 $\mu$l beads. The beads are 1 $\mu$m (in diameter) streptavidin coated silica beads and are in a solution of $9.315 \cdot 10^9$ beads/ml. The bead solution is sonicated for 20 seconds to remove clusters of beads and in the case of a sample with DNA 1 $\mu$l, 1 : 1500, will be added to the bead solution after sonication. This bead solution will then be put to rest for at least 20 minutes for the biotin on the DNA to bind to the streptavidin on the beads, but is left rotating slowly to prevent the beads from precipitating.[19]

After the sample is incubated with antibody and the DNA is linked to the beads, 30 $\mu$l of the bead solution is introduced to the sample. Next the sample is put upside down for 5 minutes in order for the beads to make contact to the surface with the objective that the antibody and antigen will bind. Then the sample is washed again with 2 times 75 $\mu$l PTC.

Finally the open ends of the channels are closed with nail polish to prevent the sample from desiccating.

When a blocking agent is used for incubating the coverslip, this will take place after the incubation with antidigoxigenin in order to prevent the blocking agent from obstructing the incubation with antidigoxigenin.

### 3.2.1 Quick Samples

Making the normal samples takes a lot of time, which makes it useful to being able to make quick samples. These quick samples can be used for a quick pilot experiment, but are less reliable than normal samples.

For making a quick sample, a microscope glass and a coverslip are cleaned with alcohol and thereafter with demineralized water and afterwards blown dry with nitrogen. Next a spacer that sticks on both sides, with a round opening in the middle, is placed on the microscope glass and the opening is filled with 15 $\mu$l PTC.

The coverslip is incubated with antidigoxigenin by adding 15 $\mu$l of the antidigoxigenin solution, made of 15 $\mu$l PTC and 5 $\mu$l antidigoxigenin stock solution, on the middle of the surface. After 20 minutes the drops are sucked up with a pipet and the surface is "washed" by adding some drops of PTC on the surface and sucking them up again with the pipet. This is done two times.

While incubating, the bead solution is made of 25 $\mu$l PTC and 5 $\mu$l beads and left rotating for at least 20 minutes. 15 $\mu$l of bead solution is added on the surface and after 5 minutes the solution is sucked up again with the pipet and the surfaced is "washed" two times.

Now the coverslip is placed on the spacer on the microscope glass with the treated side towards the microscope glass and with the treated area of the surface placed in the round opening of the spacer. The coverslip is pressed on the spacer to ensure that the sample is completely sealed and will not dry.

The quickest sample is made by cleaning a microscope glass, incubating it with antidigoxigenin the same way as the coverslip described above.

While incubating, the bead solution is made of 25 $\mu$l PTC and 5 $\mu$l beads and left rotating for at least 20 minutes. 15 $\mu$l of bead solution is added on the

surface and after 5 minutes the solution is sucked up again with the pipet and the surfaced is "washed" two times.

Then the sample is immediately analyzed using a simple light microscope. These kind of samples for quick pilot experiments.

## 3.3 Existing Data Acquisition and Analysis Programmes

### 3.3.1 Data Acquisition Program

There are two data acquisition programmes for the CFM. The first is to make a so-called kernel file and the second to obtain data. In both of the programmes it is possible to look at the sample with the camera. The focus can be changed manually or with the program. Also with both programmes regions of interest, or ROI's, consisting of 50x50 pixels should be chosen to select the beads that will be measured. This also means that a second bead in the ROI, even if it is only partially, will disturb the measurements.

When a kernel file is made, the objective is to select beads that are stuck to the surface. When the measurement is started, the program will change the focus on the beads, by moving the sample closer to the objective using a piezo. This way it is possible to make a calibration curve of the relative position of the bead in the z-direction against the light distribution of the bead, with the z-direction in the same direction of the arm of the CFM. The program measures 21 different depths of focus and takes of each depth 250 frames, with a speeds of 14 fames per second. In total the sample will be moved 10 $\mu$m during the measurement.

While obtaining data it is possible to rotate the sample with the CFM, which is also controlled by that program. At this moment the maximum rotation speed is still limited to 200 rpm, which corresponds to a maximum force of 132 fN with the used beads. It is possible to change the focus with the program during the measurements. The data again is taken with a speeds of 14 frames per second and will be saved per ROI.

### 3.3.2 Analysis Program

For the kernel files, a program exists that will take the average of all 250 frames for every depth and separately for every ROI. There is another program which allows one to look at the kernels, averaged and non-averaged, frame by frame.

For the data there is a program which allows one to look at the raw data, frame by frame. Also there is a program which will compare the data with a kernel file of choice and will calculate the relative position of the bead in the z-direction. Finally there is a program which will plot the relative position of the bead in the z-direction against the time. This program also plots the position of the bead in the x-direction and the position of the bead in the y-direction.

# Chapter 4

# Experiment

The situation in which I did my bachelor research was slightly different from normal because of two reasons.

First of all I have been absent for three weeks in the middle of my research, which was due to family reasons. Most of my time was spent on optimization of the sample preparation in that period, which is why I will mention my period of absence in section 4.2.

Second of all I worked together with a master student, Jarno ten Pierik, for a great deal of time. The objective was that he would teach me how to make samples with the existing protocol and that he would work on optimizing the analysis programs. By the time I could make the samples on my own, there was not much work left for Jarno in optimizing the analyzing programs. Therefore we did a lot of experiments together and he also did a part of the experiments on his own. When I mention in this report that Jarno has seen something or has done an experiment, I mean that he did it in my absence. All the experiments I did after returning from my period of absence, I performed without Jarno.

## 4.1 Data Acquisition and Analysis Programmes

At the start of this research project there were two different programmes, one for the kernel measurements and another for the data measurements. It seemed to be easier if both measurements could be done with one program which would allow one to use the same ROI's. This way it is possible to determine the position of the stuck beads used for the kernel file, which is an easy way to check the obtained calibration line and the analysis programmes.

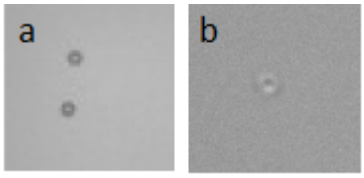


Figure 4.1: *a: a symmetric light distribution of the bead. (picture from [14]) b: an asymmetric light distribution of the bead due to the use of a non collimated light source.*

One of the problems with the analysis programmes was that there were some difficulties with the light distribution of the bead. The analysis was based on a bead with a symmetrical light distribution, as in figure 4.1a. But as it turned out when the beads

go out of focus they get an asymmetrical light distribution, as in figure 4.1b, which would cause mismatching while comparing to the kernel files.

This asymmetry is caused by the LED, of which the light is not perfectly collimated. That is the reason why the assumption was that this asymmetry would be rotational symmetric throughout the sample. There were thoughts to make different kernel files of different parts of the sample, so it would be possible to match data to kernels from the same region of the sample.

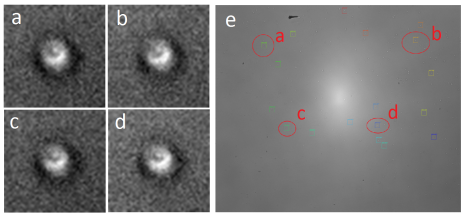


Figure 4.2: *a,b,c,d: pictures of beads from different region in the sample. e: the sample with the position of the beads from a,b,c and d marked.*

After some analysis made by Jarno the asymmetry proved to be the same for every region in the sample that is recorded, as is shown in figure 4.2. This means that one kernel file could be used for al the data.

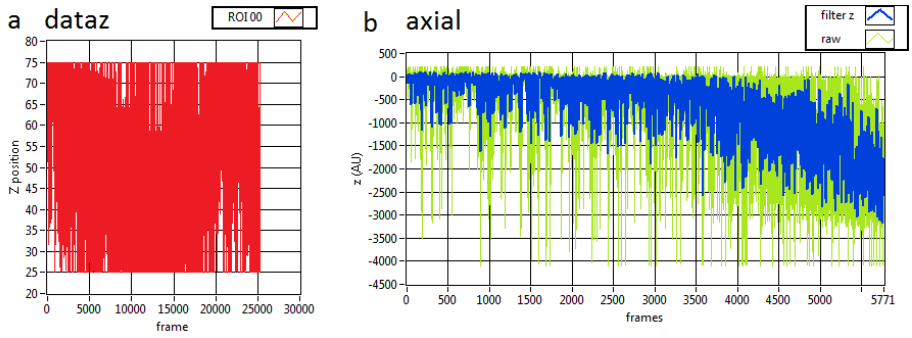


Figure 4.3: *a: two times the position of the bead in the z-direction in pixels. b: axial movement of the bead. (sample DNA1 from 06-06-2013 ROI4)*

The calculation of the position of the bead in the z-direction did not function well. Figure 4.3 shows a fit of the position of a tethered bead in the z-direction. It became clear that the problem was not one of the programmes, but was actually due to the fact that the sample holder experienced too much friction while moving. Although it is also not certain whether the analysis programmes will be able to calculate the position of the bead in the z-direction. This resulted in a movement of the sample holder that was not similar to the force exerted by the piezo: the sample holder would be stuck for some time, until the moment that the pressure of the piezo got too high and the sample holder would move a certain distance. This way there was no way of knowing how much the focus had changed, whereby it was not possible to make a calibration curve. For this reason there had to be developed a new sample holder, which takes a lot of time.

Meanwhile there had to be developed another analysis program to study the behavior of the tethered beads until the new sample holder is finished.

This new program analyzes the radial movement of the bead projected on the x,y-plane and is based on the difference in Brownian motion of the bead when its tether elongates.

After improving the search for a maximum in the light distribution, solving problems with background noise, problems with negative values and possible anti-correlation (a frame matched to the negative of the light distribution of the bead) the analyzing programmes worked satisfactorily.

## 4.2 Sample Preparation

### 4.2.1 Existing Protocol

The first samples were made with the existing protocol, but the concentration of beads on the coverslip was to high. The concentration was so high that it was not possible to select any beads in a ROI unless there were also other beads in that same ROI.

The reason for the high concentration of beads on the coverslip is that the beads stick to the surface through non-specific bonds. A blocking agent in the solution of the beads, could block the surface of the bead hereby reducing the change of non specific binding of the beads to the surface and to other beads. Incubation of the coverslip with a blocking agent will reduce the change of non-specific bindings between the coverslip and the beads.

### 4.2.2 PTC1

The first suggestion to reduce the amount of beads stuck to the coverslip was to use casein, which is in fact milkpowder, as a blocking agent. Casein was used as blocking agent before with polystyrene beads, but was suspected of causing clustering of the silica beads used in this experiment. To verify this statement a solution was made of PTC and casein with a concentration of 1 mg Casein per ml PTC, called PTC1. Quick samples were made with 45 $\mu$l PTC as a solution, 45 $\mu$l PTC1 as a solution and the coverslip incubated with PTC1 but with 45 $\mu$l PTC as a solution. The results were:

| Sample | Incubated with | Solution | result |
|---|---|---|---|
| 1 | - | 5 $\mu$l beads + 45 $\mu$l PTC | no clustering |
| 2 | - | 5 $\mu$l beads + 45 $\mu$l PTC1 | a lot of clustering |
| 3 | PTC1 | 5 $\mu$l beads + 45 $\mu$l PTC | a lot of clustering |

As it causes clustering of the beads, which means that the beads become more sticky, casein is not a suitable blocking agent.

### 4.2.3 PTC2

Bovine serum albumin, or BSA, is also a blocking agent and PTC already contains BSA in a low concentration of 20 $\mu$g/ml. Because it causes no clustering of the beads, BSA could be a suitable blocking agent. To investigate BSA as a main blocking agent, two of the quickest samples, without incubation with antidigoxigenin, were made but one of them with PTC2 instead.

Here PTC2 is PTC with 1 $\mu$g/ml extra BSA, which gives a total concentration of $1,02$ mg/ml BSA in the solution. These samples showed that this higher concentration of BSA does not cause clustering of the beads. That is why subsequently two real samples were made with PTC2, one sample with DNA and the other without DNA. Also the samples are incubated with PTC2 for 30 minutes. Figure 4.4 shows one of these samples. As is clear from this figure, the concentration on the coverslip is good and it is possible to select several beads for measurements. There is only a small amount of small clusters consisting of $2-5$ beads.

Even though there was a good concentration on the coverslip, there were only stuck beads visible.

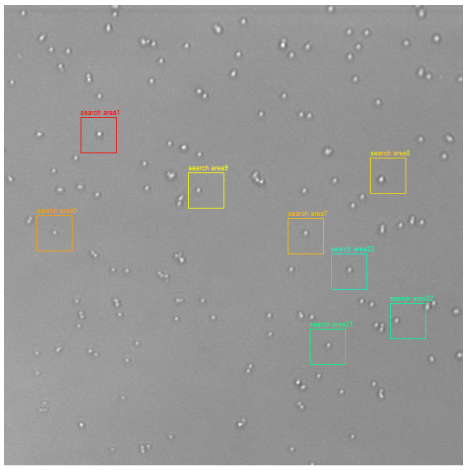

Figure 4.4: *Snapshot of a sample in PTC2 and also incubated with PTC2 (sample 2 18-02-2013).*

### 4.2.4 Coverslips cleaned with HF

There was a suggestion based on experience that antidigoxigenin attaches better to a coverslip, when its surface is first treated with HF (hydrofluoric acid). This treatment will be explained in subsection 4.2.7. For optimal effectiveness the coverslips should be used the same day as they were treated or cleaned with the HF.

First there were made two samples with PTC2 (also incubated with PTC2) and coverslips cleaned with HF, without DNA. The first sample broke, but the second had a beautiful low concentration of beads on the coverslip, see figure 4.5. It appeared that the combination of using the combination of a coverslip treated with HF and PTC2 as a blocking buffer resulted in a low concentration of beads on the coverslip, which still had to be verified by more experiments.

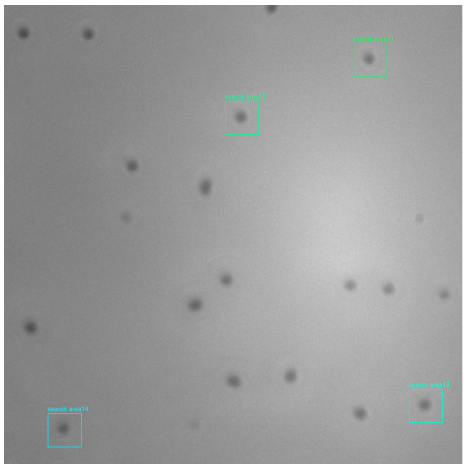

Figure 4.5: *Snapshot of a sample in PTC2, incubated with PTC2 and using etched coverslips. (sample 2 20-02-2013)*

### 4.2.5 Back to PTC

Jarno made three quick samples, one with PTC on a cleaned coverslip, one with PTC2 on a cleaned coverslip and one with PTC2 on a coverslip cleaned with ethanol and demineralized water. He incubated the coverslip for 30 minutes and he took one hour for the precipitation of the beads. He concluded that with PTC as blocking buffer almost no beads would stick to the surface of the coverslip and PTC2 would give a fine concentration of beads on the coverslip but would also cause a lot of small clusters of $2-5$ beads. This is why he concluded that PTC worked better as a blocking buffer then PTC2.

Also a new DNA stock solution was made with a slightly altered concentration, of which 2 $\mu$l is to be used for a sample in stead of 1 $\mu$l. More about this knew DNA stock in subsection 4.2.9.

When making two new quick samples with PTC and one hour precipitation time for the beads, there was a very high concentration of beads on the coverslip.

After two real samples were made with PTC and a precipitation time for the beads of one hour, it was clear that the concentration of beads on the coverslip was very high. This measurement was confirmed by the next measurement with two real samples, giving a concentration of beads as shown in figure 4.6A.

Due to these huge differences in results while making the same samples, it was important to make a lot of samples and trying to make them consistent with each other. In this period I was absent for three weeks.

Starting again after the period of absence, Jarno had changed the precipitation time for the beads to 3 minutes, which seemed to improve the concentration of the beads on the coverslip. After making several samples with this 3 minutes precipitation time, it became clear that the concentration of beads on the coverslip had indeed improved, but was still to high (see figure 4.6B). Also there were no moving beads found in the samples. This led to the conclusion that the beads were still too sticky and possibilities of a blocking agent should be reconsidered.

### 4.2.6 Back to PTC2

The suggestion was that it would be useful to investigate BSA as a blocking agent again, because BSA might have been put aside as a blocking agent too fast. Another candidate for the blocking agent was fish skin gelatin or FSG, but due to delivery problems it was not possible to do experiments with FSG.

Quick samples were made to investigate the effect of normal PTC, PTC with 1 mg/ml BSA, PTC with 5 mg/ml BSA and PTC with 10 mg/ml BSA. These samples showed that adding BSA to the PTC as a blocking buffer had a reducing effect on the concentration of beads on the coverslip, but from these experiments it was not possible to determine what concentration of BSA would be optimal.

Several normal samples were made with PTC2 and with PTC10 (which is PTC with 10 mg/ml BSA), both with 30 minutes incubation time of the blocking buffer, 3 minutes precipitation time for the beads. The samples with PTC2 showed a fine concentration of beads on the coverslip. There

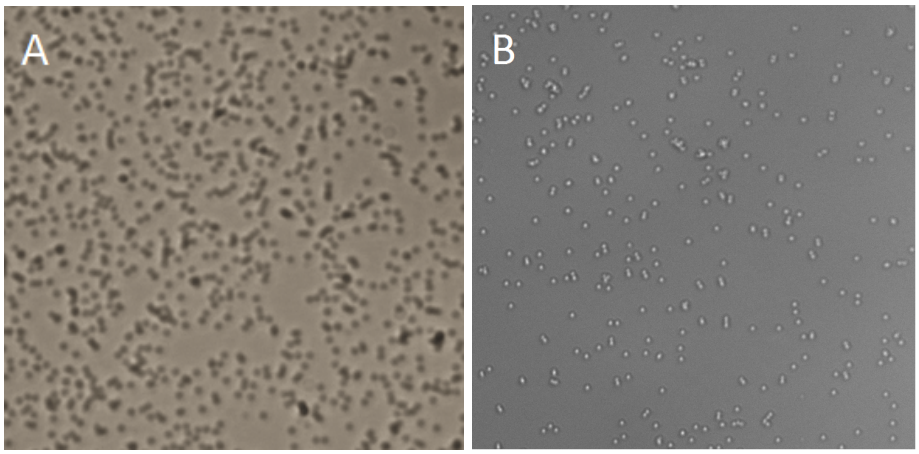


Figure 4.6: *A: Snapshot of a sample in PTC, with 1 hour precipitation time of the beads and using etched coverslip. (sample 1 12-03-2013), B:Snapshot of a sample in PTC, with 3 minutes precipitation time of the beads and using etched coverslips. (sample 1 26-04-2013)*

were several small clusters of $2-5$ beads, but there were also several single beads. The samples with PTC10 had a fine concentration as well, but most of the beads were in clusters of $2-5$ and there were barely any single beads. This led to the conclusion that PTC2 was more suitable as a blocking agent then PTC10.

Making the samples with DNA using PTC2 as blocking buffer, including 30 minutes of incubation time of the blocking buffer and using 3 minutes for the beads to precipitate gave samples with a good concentration of beads on the coverslip, as is shown in figure 4.7. These sample contained a few moving beads each and due to the low concentration it was possible to select these beads for measurements. When making several samples, the concentration of beads on the coverslip would fluctuate a bit, but all the samples were fit for measurements.

This led to the final protocol, which is presented in appendix A and appendix B for respectively samples with DNA and samples without DNA.

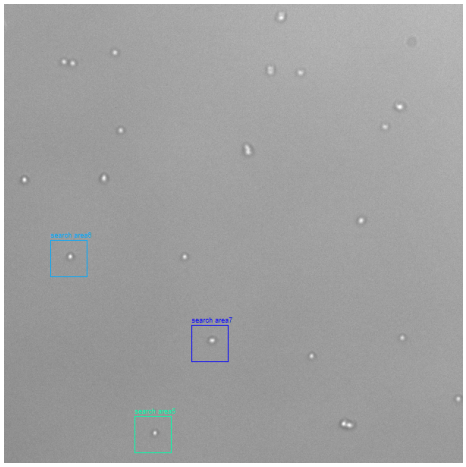

Figure 4.7: *Snapshot of a sample in PTC2, incubated with PTC2, with 3 minutes precipitation time of the beads and using etched coverslips. (sample DNA 31-05-2013)*

### 4.2.7 Cleaning Coverslips with HF

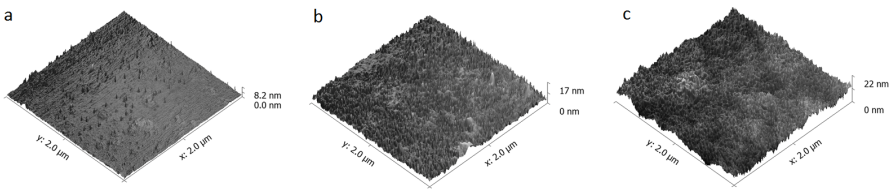


Figure 4.8: *Atomic Force Microscope image of High Resolution coverslips, a: not treated, b: treated with HF for 1 minute, c: treated with HF for 4 minutes.*

Hydrofluoric acid is highly corrosive and has the ability to etch the glass. The effect of HF on a glass coverslip is shown in figure 4.8. It should be noted that the coverslips used in the figure are High Resolution coverslips and in this experiment normal coverslips are used, but the effect remains the same. Also notable is that the scale of the z-direction is in nm and the scale of the x-direction and y-direction is in $\mu$m.

In this experiment the coverslips are treated with 8% HF for 1 minute. Afterwards they are cleaned in demineralized water twice and stored in demineralized water.

When etched with HF, the top layer of the coverslip is removed, including the pollution of the surface of the coverslip. What remains is a surface which is less susceptible for non-specific binding.

When working with HF one should be extremely cautious, HF is very corrosive and a contact poison. Burnings caused by HF could display themselves only after $1 - 2$ days, which results in possible delay of important treatment. After exposure HF reacts with the calcium in the body, which could cause cardiac arrest.

### 4.2.8 Calculations on Beads and BSA

According to the manufacturer there are $9,315 \cdot 10^9$ beads/ml in the stock solution, there are $9.268 \cdot 10^{11}$ beads per gram of dry particles, 1 g of beads has a total surface of $9.268 \cdot 10^{12}$ $\mu$m$^2$ and that it takes 3 mg BSA to create a monolayer on a surface of 1 m$^2$. [19] [20]

According to this data 5 $\mu$l beads contains 50.3 $\mu$g beads with a total surface of $4.66 \cdot 10^2$ mm$^2$. For this surface 1.40 $\mu$g BSA is needed to create a monolayer around all the beads, which theoretically means that the bead is completely blocked for non-specific bindings.

The surface of the coverslip situated in the channel of the sample is $5mm \times 22mm = 110mm^2$, which means 0.33 $\mu$g BSA is needed to create a monolayer on the coverslip.

This means that a total amount of 1.73 $\mu$g BSA is needed to create a monolayer on the surface of the coverslip and around all the beads in one sample.

According to the manufacturer of the parafilm used in the experiments, the parafilm has a thickness of 127 $\mu$m[21]. This gives the channel of a sample a volume of $110mm^2 \times 0.127mm = 14.0mm^3 = 0.014ml$. As PTC2 contains in total 1.02 mg/ml BSA, the channel of the sample filled with PTC2 contains 14.3 $\mu$g, which is a factor 8 more BSA then is needed to create a monolayer on the surface of the coverslip and around all the beads. Although one should assume that not al the BSA in the channel will block the surface of the coverslip or the beads, one could assume this amount of BSA is enough to create a monolayer on the complete surface.

Because the channel of the sample has a surface of $5mm \times 22mm$ and 1 $\mu$m beads are used in this experiment, $1.1 \cdot 10^9$ beads are needed to create a monolayer on the coverslip. The 5 $\mu$l bead stock solution used in this experiment contains $4.66 \cdot 10^7$ beads.

### 4.2.9 Calculations on DNA and Beads

During the experiment the objective is that the majority of the beads is tethered. The beads are not allowed to be tethered by two DNA strands at the same time, because then the dynamics of a whole different system is analyzed. And because it is probably hard or maybe even impossible to tell apart beads that are tethered by one or by two strands of DNA, it is desired that the amount of beads in the solution with two DNA strands attached is negligible.

The distribution of the DNA strands among the beads is determined by the poisson distribution, with as mean value the ratio of DNA/beads in the solution. There must be determined an optimal ratio DNA/beads, where as much beads as possible have a DNA strand attached but as little beads have possible are more then one DNA strands attached. The preference was that $95 - 98\%$ of the beads with a DNA strands attached, should solely have one DNA strand attached.

According to the poisson distribution this means the DNA/bead ratio should be 1/10-1/50.

When making a new stock solution of DNA the ratio DNA/beads was considered, but also the amount of solution that would be used during the experiments. The experience was that taking 1 $\mu$l with a pipet was rather inexact but also the stock solution should not be to diluted. For this reason a DNA stock solution of 1 : 5000 was made and in the experiments 2 $\mu$l of this solution would be used. This would give a DNA/bead ratio of 1/19, compared to the ratio DNA/beads 1/12 used before.

Considering the size of the bead compared to the size of the DNA strand, it is not always possible for a second attached strand on a bead to reach the surface of the coverslip, simply because it is not long enough. If one DNA strand is attached to a bead, almost half of the surface of the bead is available for a second DNA strand to be attached without being able to also attach to the coverslip.

### 4.2.10 Calculations on Bead Movement

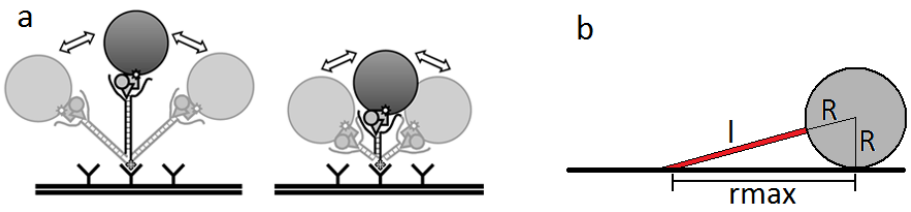


Figure 4.9: *a: a tethered bead displaying Brownian motion. (picture from [16]) b: a bead at its maximum exertion.*

Because a tethered bead is not stuck to the surface and there is a certain amount of thermal energy available, the bead will move as is shown in figure 4.9a. The movement of the bead is the Brownian motion. As one can see in figure 4.9b, the maximum distance $r_{max}$ that a bead will move, projected on the x,y-plane like one would observe when using a microscope, is given by $\sqrt{(l+R)^2 - R^2} = \sqrt{l^2 + 2lR}$. Here $l$ is the length of the DNA strand and R is the radius of the bead.

In this case, this gives $r_{max} = 429nm = 2.5pixels$ (rounded at 2 significant figures this value is the same for telomere DNA and ILPR).

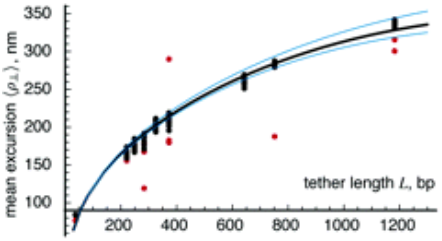


Figure 4.10: *Graph with on the x-axis the length of the tether in nm and on the y-axis the average radial movement in nm. The dots are measurements and the curve is a fitted line. The used beads are 480 nm in diameter. (picture from [22])*

Still it is not probable that the bead will actually move to what is physically possible. There is a way to make an estimation of the average excursion of the bead $< r >$. Figure 4.10 shows a graph that plots the mean excursion in nm against the tether length in nm (the graph says the tether length is in base pairs, but comparing the graph with other graphs from the same paper makes it evident that the tether length should be in nm)[22]. This graph is based on a bead of 0.48 $\mu$m, which is a little less then half of the size of the bead used in this experiment. It is not probable that a bead half of the size would move twice as much, but it is probable that the whole system could be scaled with a factor 2. This means that in this graph the value of $< r >$ belonging to a tether length of 210 nm, which is about half the length of the tether used in this experiment, is half of the value of $< r >$ for the tethered bead in this experiment.

The value of $< r >$ for the tethered beads used in this experiment will then be $200nm = 1.2pixels$.

## 4.3 Measurements on Tethers

Once the samples had a concentration that was low enough to measure separate beads, every sample contained moving beads. The number of (measurable) beads varied between $1 - 8$ beads per sample.

In al the radial graphs there has been a correction for the linear drift, which is visible in the x- and y-direction graph.

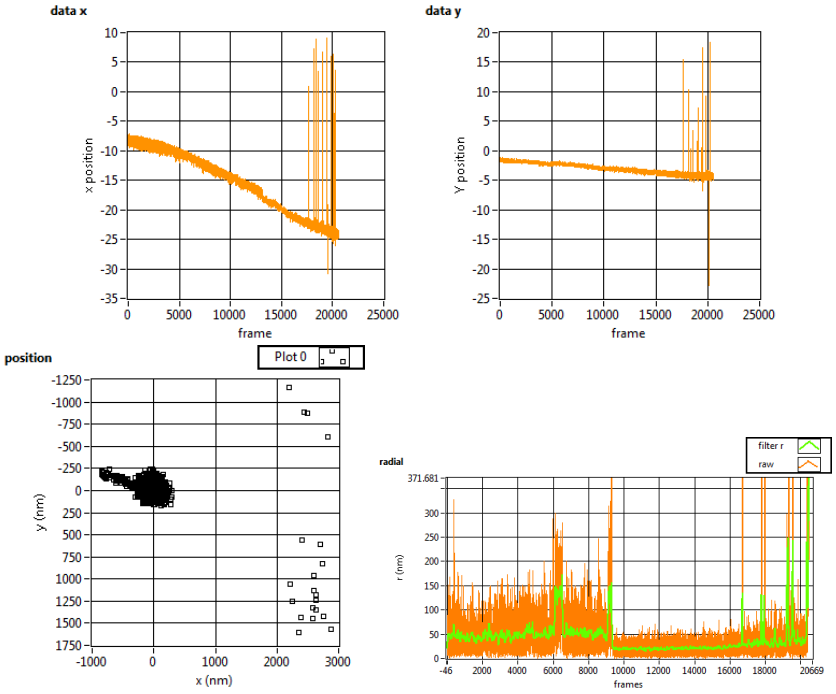


Figure 4.11: *Sample made with the final protocol. Upper left: 2 times the position of the bead in the x-direction in pixels, upper right: 2 times the position of the bead in the y-direction in pixels, lower left: position of the bead in the x,y-plane in nm, lower right: radial position of the bead in nm. (Sample DNA 28-05-2013 ROI0)*

Figure 4.11 shows the results of one of the beads measured in the first successful measurements on moving beads. The x- and y-position show a linear drift over time, the x-position more then the y-position. The linear drift is the same in the average position as in the actual position. The position graph shows a few mismatches on the right and a sort of "attached arm" on the left, but when looking closer to the position graph, at figure 4.12, it is clear that the "attached arm" on the left does not contain a lot of data points. When looking at the radial graph, there is an average movement of about 60 nm in the first part, while it increases two times to about 125 nm. The second part of the measurement the radial position stays at about 20 nm.

The data in figure 4.13 shows a huge movement in the x- and y-direction of

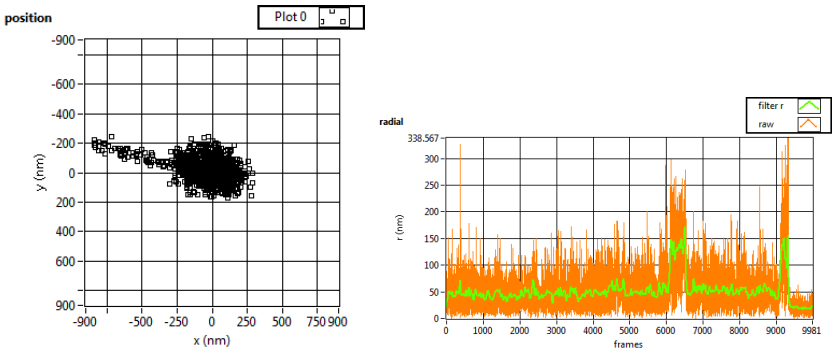


Figure 4.12: *Sample made with the final protocol. Left: position of the bead in the x,y-plane in nm, right: radial position of the bead in nm. (Sample DNA 28-05-2013 ROI0)*

the bead in the middle part of the measurement, which is also visible in the graph of the radial movement. This movement is around 1250 nm. Also there is a linear drift visible in the x- and y-direction although the actual movement in the y-direction does not follow that linear drift. The position graph clearly shows two separated sets of data points.

The data in figure 4.14 shows linear drift in the x- and y-direction, the actual movement in the x- and y-direction follow this drift. Also there are some changes in drift and one big step in the drift in the y-direction. The position graph shows a round distribution. The radial graph, which is enlarged in 4.15, shows in the first part of the measurement movement of around 190 nm with two fall backs to around 90 nm. In the middle part of the measurement the radial graph shows a movement of around 20 nm and in the last part of the measurement of around 50 nm.

Figure 4.16 shows a linear drift in the x- and y-direction, the actual movement also displays this drift. The position graph shows a round distribution of data points with only a few data points outside this disk. The radial graph shows a movement of about 20 nm.

In most of the data the beads showed an average radial movement between $70 - 120$ nm or around the 20 nm. Also several beads showed radial movement of around 1000 nm or more.

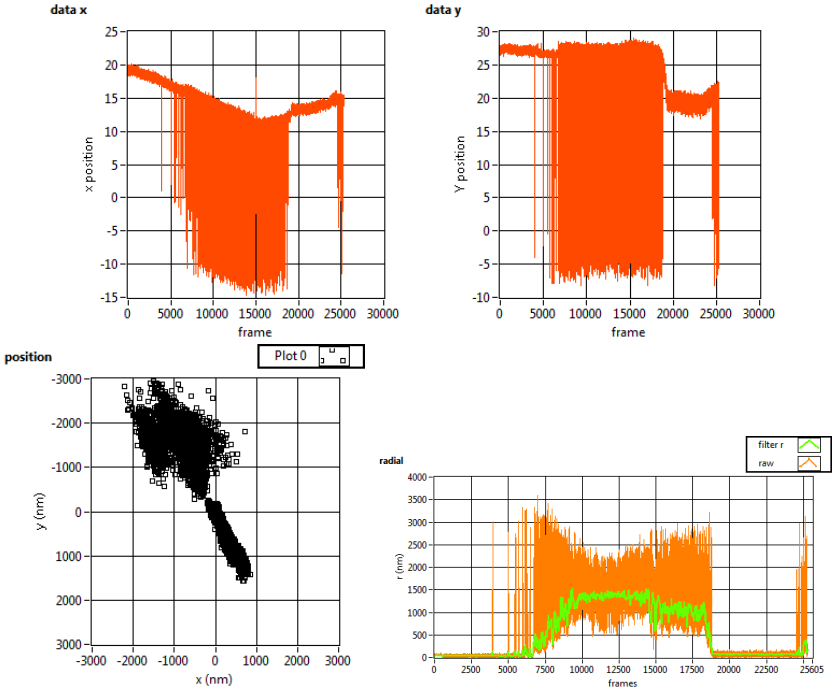


Figure 4.13: *Sample made with the final protocol. Upper left: 2 times the position of the bead in the x-direction in pixels, upper right: 2 times the position of the bead in the y-direction in pixels, lower left: position of the bead in the x,y-plane in nm, lower right: radial position of the bead in nm. (Sample DNA 06-06-2013 ROI1)*

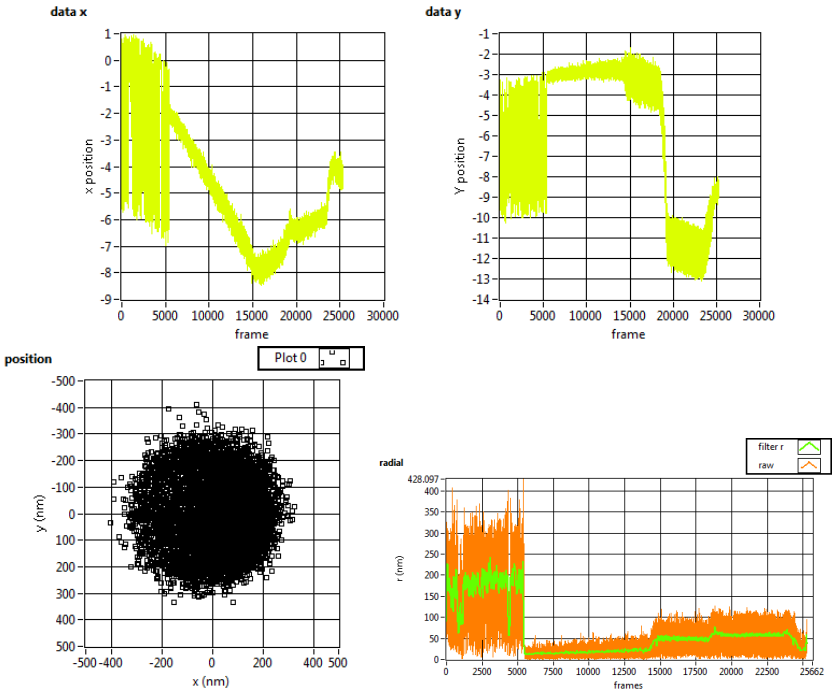


Figure 4.14: *Sample made with the final protocol. Upper left: 2 times the position of the bead in the x-direction in pixels, upper right: 2 times the position of the bead in the y-direction in pixels, lower left: position of the bead in the x,y-plane in nm, lower right: radial position of the bead in nm. (Sample DNA 06-06-2013 ROI4)*

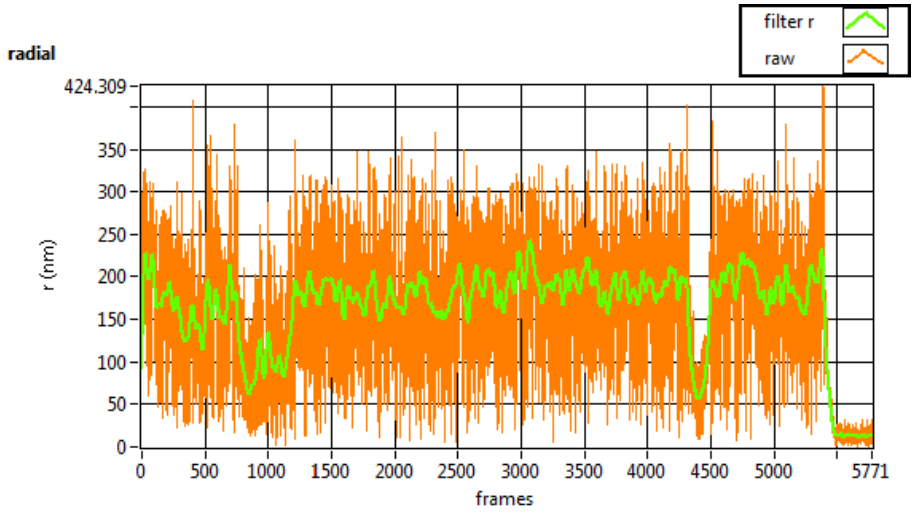


Figure 4.15: *Sample made with the final protocol. Radial position of the bead in nm. (Sample DNA 06-06-2013 ROI4)*

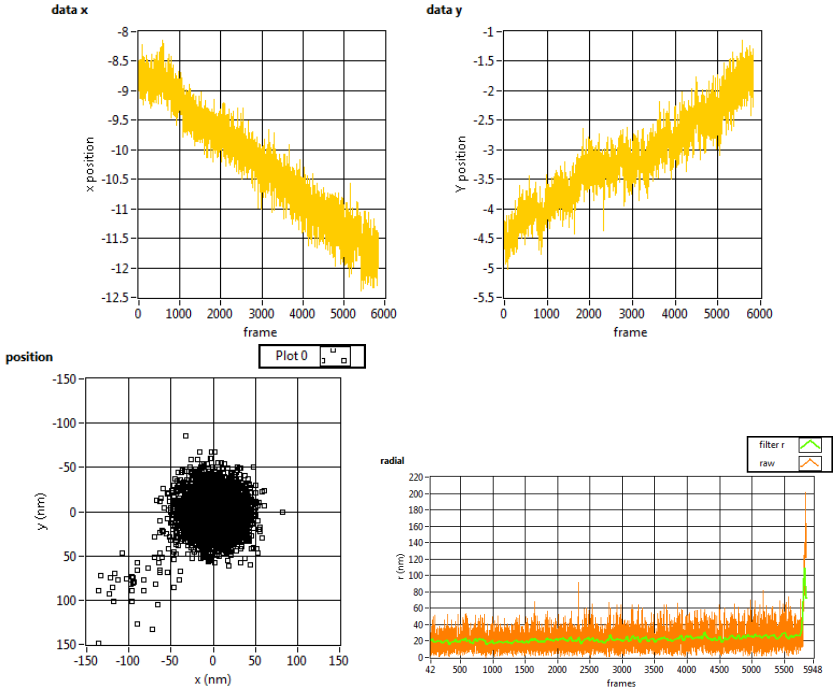


Figure 4.16: *Sample made with the final protocol. Upper left: 2 times the position of the bead in the x-direction in pixels, upper right: 2 times the position of the bead in the y-direction in pixels, lower left: position of the bead in the x,y-plane in nm, lower right: radial position of the bead in nm. (Sample DNA1 07-06-2013 ROI1)*

# Chapter 5

# Conclusions and Discussion

## 5.1 Measurements

As is explained in section 3.1 the expected elongation of the telomere DNA is 66 nm. This is when all three of the G-quadruplexes unfold at the same time. It is also possible that only one G-quadruplex unfolds, which would give an elongation of 22 nm.

When measuring on a telomere with three G-quadruplexes it is possible that the observed dynamics are not the behavior of three times a single quadruplex, it could be that the quadruplexes influence each other. It is also possible that the observed DNA strand forms only one quadruplex consisting of both endings of the sequence, which would then form a "$3 + 1$" bimolecular G-quadruplex. This would be the most common configuration for a three repeat telomere according to some research[23]. Off course this kind of telomere would also have a different dynamical behavior then a monomolecular G-quadruplex.

The expected time-scale in which the unfolding of the G-quadruplexes takes place is several seconds. This estimation is based on experiments that show that unfolding of double-stranded DNA loops unfold and fold on a time-scale of minutes[24]. Because single-stranded DNA is softer then double-stranded DNA, the expected time-scale for the unfolding and folding of single-stranded DNA is shorter.

The forces exerted on molecules in a cell are known to be up to 10 pN. Because of the expected regulating role of the G-quadruplexes, the G-quadruplexes are expected to completely unfold within this region of force and they are expected to be stable or more or less stable in the region where the force is proportional to the thermal energy. This thermal energy of double stranded DNA is proportional to a force of around 4 pN.

During this study, there was a paper of another research group describing the mechanical unfolding of G-quadruplexes[13]. It was also the aim of this study. In the paper magnetic tweezers were used to exert the force on the quadruplex and FRET was used to analyze the behavior of the quadruplex. The DNA used was telomere DNA and the used solution contained $Na^+$ and not $K^+$. The paper describes the folding and unfolding of the quadruplex on

the time-scale of seconds (see figure 5.1), as we expected. The force necessary to unfold the quadruplex is smaller then we expected, but this measurement is taken in a sodium solution. The paper also shows that the quadruplex is more stable in a potassium solution, which also corresponds with our expectations.

The data showed that a lot of beads had an average radial movement between $50 - 120$ nm. As explained in subsection 4.2.10 the average radial movement of a fully tethered bead should be around 200 nm, which is $2 - 3$ times as much. This means that these beads are not fully tethered. At this moment it is not possible to observe in what state these beads are. One possible explanation could be that the handle with the digoxigenin at its end is stuck to the surface, but that the other handle is not. But this would not explain the *range* of $50 - 120$ nm in movement.

The beads that show an average radial movement around 20 nm are probably stuck beads. This 20 nm should be the standard deviation $\sigma$ of the measurements.

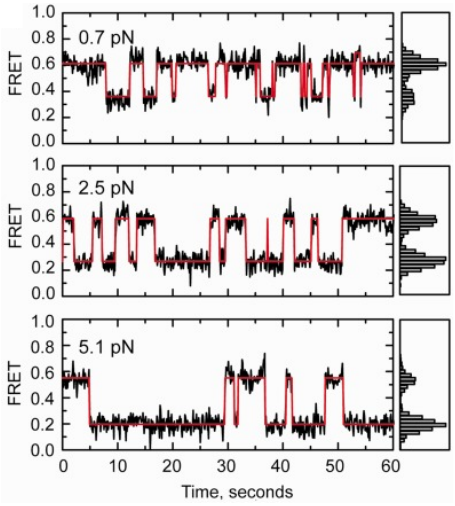


Figure 5.1: *Dynamical behavior of a tethered bead while exerting a force using magnetic tweezers, in a FRET measurement. (picture from [13])*

The data of graphs in figure 4.11 an 4.12 gave hope in a tethered bead possibly even showing some unfolding and folding because of the short steps in average radial movement of 60 nm, but as explained the average radial movement of a tethered bead in the folded state should be around 200 instead of 60 nm. The graphs of the position in the x- and y-direction show some mismatches in the end of the measurement and also the position graph shows some data points that are not in the same region as the majority of the points. The distribution of this majority of the data points is almost a disc, which is a good sign

The graphs of the position of the x- and y-direction in figure 4.13 show that there is a lot of mismatching in the middle of the measurement, because it is impossible for a bead to move $10 - 15$ pixels, which is equivalent to $1720 - 2580$ nm. The disturbance could have come from something on the side of the ROI, because from the middle to the side is 25 pixels away from the side and the bead was not exactly in the middle of the ROI. Also the position graph shows a distribution which is not expected for a bead. The data points of expected movement would form a disk since random (Brownian) movement is expected. The radial graph shows an average movement around 1200 nm, which is physically not possible for a tethered bead.

The graph of the position in the x- and y- direction of figure 4.14 shows a reasonable movement in the first part of the measurement. This movement is also visible in the radial graph of figure 4.14 and 4.15. The movement is

around 190 nm, which means this is probably a fully tethered bead. In the middle part of the measurement the average radial movement is around 20 nm, which means the bead is stuck. In the last part of the measurement the average radial movement increases to $50 - 60$ nm, which means that the bead does not become fully tethered again. The position graph shows that the distribution of data points describe a disk, which confirms that this was a good measurement.

The graphs in figure 4.16 show a nice example of a stuck bead. There is not much special shown in the graphs of the x- and y-direction. The radial graph shows a steady movement around 20 nm, which probably displays the standard deviation in the measurement. The position graph shows a nice disk containing most data points and only a few mismatched data points outside this disk.

## 5.2 Sample preparation

The sample preparation has been greatly improved.

It is now possible to make samples with a concentration that is low enough for beads to be selected in a ROI for measurements. Also the samples contain moving beads, which is great news.

The concentration of beads on the coverslip still fluctuates between different samples. This could be a result of lack of training, but the consistency of the samples should be improved.

As stated in section 5.1, the beads do not move as much as they should when completely tethered (except for one bead for a small amount of time). This could mean that the beads are still a bit to sticky, which is also confirmed by the fact that there are quite a lot of double beads in the sample.

It still takes a lot of time to make a sample.

## 5.3 Data Acquisition and Analysis Programmes

The data acquisition and analyzing programmes have been improved.

It is now possible to use the same ROI's for recording data and for kernel measurements.

The analysis programmes are not optimal yet. There is still a lot of mismatching. Further the determination of the radial position has been a great improvement but the addition of the determination of the position in the z-direction of the bead would be very useful. Still using and evaluating the method for determining this position is only possible if there is a better sample holder which does not experience resistance while being moved and which is more stable.

It would also be useful if the graphs could be exported in an easy way.

## 5.4 Suggestions for Further Research

When there is a new sample holder it will be possible to evaluate and improve the determination of the position of the bead in the z-direction. This will also

give a great addition on the information about the behavior of an observed tether in the sample.

With the new sample holder it will also be possible to use the new sample, which has the coverslip on the downside and a closed channel with excess through two small tubes sticking trough the microscope glass. This will make it easier to wash the sample and this sample will not have to be put upside down while incubating. Hopefully this method will also give more consistency among the samples.

It might be useful to investigate whether sonication has a destroying influence on the streptavidin of the bead and whether it is really necessary to use sonication.

The effect of the concentration of $K^+$ could be explored and the effect of replacing $K^+$ with $Na^+$.

It would be interesting to measure with higher rotational speed and to use heavier beads in order to increase the force exerted on the beads.

It would be very interesting to do measurements on ILPR and on other sequences in the promotor region of important genes and on RNA. Knowledge about the dynamical behavior of these parts of DNA and the manipulation of this behavior could be of enormous value for research on curing for instance diabetes type 1.

In the future the effect of G-quadruplex specific drugs on the stability of the quadruplexes can be tested.

# Chapter 6

# Acknowledgements

First I would like to express my gratitude to my supervisor, Dr. Gerhard Blab, who has supported me throughout my research and who was always there to give me a helping hand.

I would like to thank Jarno ten Pierik for initially teaching me how to make the samples and for his assistance with part of the experiments.

Also I thank Jarno ten Pierik and Gerhard Blab for the use of the programmes for data acquisition and analysis in my research. They have written these programmes and they have made the necessary improvements to them throughout my research.

My gratitude also goes to Dave van den Heuvel for his help and advice whenever I needed it. Also I thank him for the use of his Atomic Force Microscopy pictures of the High Resolution coverslip (figure 4.5) in my thesis.

I would like to express my appreciation to Qiao Li and my mother. They both read the manuscript of my thesis and helped correcting and improving it.

Finally I wish to thank the Molecular Biophysics Group at Utrecht University for their support and company. I really had a great time while conducting my research there.

# Appendices

# Appendix A

# Protocol with DNA

| Timing | | | Description |
|---|---|---|---|
| In advance | 1 | | Make 1,5 ml PTC2*<br>(1,5 ml PTC + 1,5 mg BSA) |
| | 2 | Cleaning slide / or take from stock** | Wash microscope glass with ethanol<br>wash microscope glass with $H_2O$<br>Blow dry with $N_2$ |
| | 3 | Make template | Cut parafilm using template<br>Put on microscope slide<br>Put coverslip on top, heat and press |
| Sample | 1 | Filling sample | Fill sample with Na buffer (20mM) |
| | 2 | Antibody solution | In eppy:<br>7 $\mu$L antidigoxigenin<br>in 21 $\mu$L Na buffer (20mM)*** |
| | 3 | | Add 20 $\mu$L antidig solution<br>Drop on both endings of channel |
| | 4 | 20 min. upside down | |
| | 5 | | wash 2 x 75 $\mu$L PTC |
| | 6 | 30 min. upside down with blocking agent | Add 75 $\mu$L PTC2<br>Drop on both endings of channel |
| | 7 | | Wash 2x75 $\mu$L PTC2 |
| Bead solution | 1 | DNA bead solution | In eppy:<br>23 $\mu$L PTC2 + 5 $\mu$L beads |
| | 2 | Sonication $\pm$ 20 sec. | |
| | 3 | | + 2 $\mu$L DNA |
| | 4 | Rotating $\pm$ 20 min. | |
| Filling Sample | 1 | DNA bead solution | Add 30 L bead DNA bead solution |
| | 2 | 3 min. upside down | |
| | 3 | | Wash 2 x 75 $\mu$L PTC2 |
| | 4 | | Close endings of channel with nail polish |
| | 5 | | Cover coverslip on both sides of channel with strip of parafilm |

*PTC2=PTC with an addition of 1 mg BSA per ml PTC
**Coverslips should be treated with HF form 1 minute and also blown dry with $N_2$

***20 mM sodium phosphate buffer at pH 8

# Appendix B

# Protocol without DNA

| Timing | | | Description |
|---|---|---|---|
| In advance | 1 | | Make 1,5 ml PTC2*<br>(1,5 ml PTC + 1,5 mg BSA) |
| | 2 | Cleaning slide / or take from stock** | Wash microscope glass with ethanol<br>wash microscope glass with $H_2O$<br>Blow dry with $N_2$ |
| | 3 | Make template | Cut parafilm using template<br>Put on microscope slide<br>Put coverslip on top, heat and press |
| Sample | 1 | Filling sample | Fill sample with Na buffer (20mM) |
| | 2 | Antibody solution | In eppy:<br>7 $\mu$L antidigoxigenin<br>in 21 $\mu$L Na buffer (20mM)*** |
| | 3 | | Add 20 $\mu$L antidig solution<br>Drop on both endings of channel |
| | 4 | 20 min. upside down | |
| | 5 | | wash 2 x 75 $\mu$L PTC |
| | 6 | 30 min. upside down with blocking agent | Add 75 $\mu$L PTC2<br>Drop on both endings of channel |
| | 7 | | Wash 2x75 $\mu$L PTC2 |
| Bead solution | 1 | Bead solution | In eppy:<br>23 $\mu$L PTC2 + 5 $\mu$L beads |
| | 2 | Sonication $\pm$ 20 sec. | |
| | 4 | Rotating $\pm$ 20 min. | |
| Filling Sample | 1 | Bead solution | Add 30 L bead bead solution |
| | 2 | 3 min. upside down | |
| | 3 | | Wash 2 x 75 $\mu$L PTC2 |
| | 4 | | Close endings of channel with nail polish |
| | 5 | | Cover coverslip on both sides of channel with strip of parafilm |

*PTC2=PTC with an addition of 1 mg BSA per ml PTC
**Coverslips should be treated with HF form 1 minute and also blown dry with $N_2$
***20 mM sodium phosphate buffer at pH 8

# Appendix C

# Constituents of PTC

For 1 liter PTC

| | |
|---|---|
| 2.422 g | Tris |
| 9.693 g | KCl |
| 0.8132 g | $MgCl_2$ + 6 $H_2O$ |
| 0.03722 g | EDTA |
| 0.02000 g | BSA |
| 0.08000 g | Heparin |

Ad 1 l 18.2 MΩ pure water (Millipore)

# Bibliography


[1] I. Bang, "Untersuchungen über die Guanylsäure," *Biochemische Zeitschrift*, vol. 26: 293-311, 1910.

[2] M. Geller *et al.*, "Helix formation by guanylic acid," *Proceedings of the National Academy of Sciences*, vol. 48 (2): 213-218, December 1962.

[3] J. L. Huppert, "Four-stranded nucleic acids: Structure and targetting of G-quadruplexes," *The Royal Society of Chemistry*, vol. 37: 1375-1384, 2008.

[4] T. M. Bryan and P. Baumann, "G-quadruplexes: from guanine gels to chemotherapeutics," *Molecular Biotechnology*, vol. 49: 198-208, 2011.

[5] G. Biffi *et al.*, "Quantitative visualization of DNA G-quadruplex structures in human cells," *Nature Chemistry*, vol. 1548, January 2013.

[6] "http://www.tutorhelpdesk.com/homeworkhelp/biology-/structure-of-dna-assignment-help.html,"

[7] L. Oganesian and J. Karlseder, "Telomeric armor: the layers of end protection," *Journal of Cell Science*, vol. 122: 4013-4025, 2009.

[8] A. Burge *et al.*, "Quadruplex DNA: Sequence, topology and structure," *Nucleic Acids Research*, vol. Vol. 34, No. 19: 5402-5415, August 2006.

[9] C. Schaffitzel *et al.*, "In vitro generated antibodies specific for telomeric guanine-quadruplex dna react with stylonychia lemnae macronuclei," *Proceedings of the National Academy of Science*, vol. Vol. 89, No. 15: 85728577, July 2001.

[10] "http://en.wikipedia.org/wiki/g-quadruplex,"

[11] "http://barleyworld.org/sites/default/files/figure-07-25.jpg,"

[12] "http://www.personal.kent.edu/ hmao/lasertweezers.html,"

[13] X. Long *et al.*, "Mechanical unfolding of human telomere G-quadruplex DNA probed by integrated fluorescence and magnetic tweezers spectroscopy," *Nucleic Acids Research*, vol. Vol. 41, No.4, January 2013.

[14] K. Halvorsen and W. P. Wong, "Massively parallel single-molecule manipulation using centrifugal force," *Biophysical Journal*, vol. vol. 34, no. 19: 5402-5415, 2006.

[15] J. Marsman, "Sample preparation to study the effects of tension on the dynamical behavier of the G-quadruplex DNA," *Bachelor Thesis*, July 2012.

[16] M. Spies *et al.*, "DNA helicases," *McGraw Hill YB of Science and Technology*, August 2002.

[17] Z. Yu *et al.*, "ILPR G-quadruplex formed in seconds demonstrate high mechanical stabilities," *Journal of the American Chemical Society*, vol. 131: 1876-1882, Januari 2009.

[18] P. Catasti *et al.*, "Structure-function correlations of the polymorphic region," *Journal of Molecular Biology*, vol. 264: 534-545, 1996.

[19] "Streptavidin coated silica microspheres; certificate of analysis," *Bangs Laboratories, Inc*, Febuary 2013.

[20] "Adsorption to microspheres, tech note 204," *Bangs Laboratories, Inc.*

[21] "http://www.2spi.com/catalog/supp/parafilm.php,"

[22] P.C.Nelson *et al.*, "Tethered particle as a diagnostic of DNA tether length," *Journal of Physical Chemistry*, vol. 110: 17260-17267, 2006.

[23] D. J. Patel *et al.*, "Human telomere, oncogenic promoter and 5'-UTR G-quadruplexes: Diverse higher order DNA and RNA targets for cancer therapeutics," *Nucleic Acids Research*, vol. Vol. 35, No. 22: 7429-7455, October 2007.

[24] Y. Chen *et al.*, "Femtonewton entropic forces can control the formation of protein-mediated DNA loops," *Physical Review Letters*, vol. 104: 048301, January 2010.

[25] A. Siddiqui-Jain *et al.*, "Direct evidence for a G-quadruplex in a promoter region and its targeting with a small molecule to repress c-MYC transcription," *Proceedings of the National Academy of Science*, vol. Vol. 99, No. 18: 1159311598, September 2002.